Breast Cancer: Targets and Therapy

Dovepress
Taylor & Francis Group

Open Access Full Text Article

ORIGINAL RESEARCH

IFI44 Orchestrates an IL-10–Driven M2 Macrophage Program in Breast Cancer: An Immune Prognostic Signature

Jiahui Wu[1,*], Wang Yi[1,2,*], Mengting Liu[1,2,*], Yingliang Li[2], Boxuan Zhou[2], Ziyun Wu[1], Wei Cao[2], Qingfeng Shi[1], Xiangkai Cai[1], Haiwei Xiong[2]

[1]The First Clinical Medical College of Nanchang University, Nanchang University, Nanchang, People's Republic of China; [2]Department of Breast Disease Center, The First Affiliated Hospital of Nanchang University, Nanchang, People's Republic of China

*These authors contributed equally to this work

Correspondence: Haiwei Xiong, Department of Breast Disease Center, The First Affiliated Hospital of Nanchang University, Nanchang, People's Republic of China, Email xionghaiwei1987@163.com

Background: Although IFI44 is recognized for its crucial role in autoimmune disorders, its function in breast cancer (BC) remains unclear. This study aimed to investigate the immune-related and prognostic significance of IFI44 in BC.

Methods: Bio-informatics analysis and in vitro experiments were performed to assess BC cells' proliferation, migration, and invasion. Immune cell infiltration was analyzed using CIBERSORT and ESTIMATE algorithms. The correlation between IFI44 and M2 macrophage markers was validated via TIMER2 and GEPIA2 databases. An IFI44-related M2 macrophage signature (IMS) was constructed using LASSO Cox regression. Its prognostic performance and association with immunotherapy/chemotherapy response were evaluated using survival analysis, ROC curves, and drug sensitivity data (GDSC2).

Results: IFI44 was highly expressed in BC and associated with poor prognosis. Down-regulation of IFI44 BC cells inhibited M2 macrophages proliferation, but exogenous IL-10 in the knockdown-IFI44 BC cells rescued this reduction in vitro. The constructed IMS, based on four genes (GPR171, KIR2DS4, NPAS1, CD79A), effectively predicted the overall survival (OS) of BC patients with high specificity and sensitivity. Of note, the IMS was applied in pan-cancer and we found it could accurately predict the prognosis and immune score in multiple cancers.

Conclusion: IFI44 promotes BC progression and M2 macrophage infiltration via an IL-10-mediated mechanism. IFI44 represents a promising target for immunotherapy in breast cancer. Our investigation identified that IFI44-based IMS provides a predictive scenario to determine the treatment and prognosis of cancer patients.

Keywords: breast cancer, IFI44, M2 macrophages, IL-10, prognosis, IFI44 related M2 macrophages signatures

Introduction

BC poses a complex health challenge, marked by its prevalence and high fatality rates, to women's wellbeing across the world,[1] and is predicted to occur in 1 in 8 women, the leading cause of mortality among females.[2] Conventional therapeutic method comprising operations; chemical treatments; radiation; hormone treatment; and precision medicine, although there have been notable improvements in BC therapy, these treatments are often linked to severe side effects, and death rate is still high.[3,4] In this situation, immunotherapies and targeted treatments with greater effectiveness and precision have emerged as promising strategies to fight BC. Some new immune checkpoints such as LAG-3, TIM-3, TIGIT, as well as signaling pathways such as JAK/STAT, MAPK, PI3K/AKT/MTOR,[5] have solved the problem of low response rate and drug resistance, but the specific mechanism of action is still unclear. Therefore, in order to find more effective immunotherapies, it is crucial to uncover novel and robust predictive biomarkers and explore the underlying mechanisms.

https://doi.org/10.2147/BCTT.S579301
Received: 16 November 2025
Accepted: 25 March 2026
Published: 8 April 2026

Interferon-induced protein 44 (IFI44) activated by type I interferons such as IFNα and IFNβ,[6] was firstly identified as a hepatitis C virus-related microtubule-clustering protein extracted from the liver cells of infected chimpanzees[7] and thought to be included in the immune response and to function upstream or downstream of the bacterial presence. In addition, the OS of patients with high levels of IFI44 was significantly lower than in those with low levels of IFI44 in HNSC.[8] Studies conducted have revealed that IFI44 is an important factor in immune diseases.[9–11] IFI44 contributes to immune cell recruitment, highlighting its potential as a therapeutic target. Yet, there is a lack of knowledge concerning on IFI44's role in invasion of immune cells in BC.

Macrophages are key components of the immune microenvironment in BC and significantly contribute to tumor progression by promoting aggressive cell behaviors in different cancers.[12,13] In solid tumor studies, tumor associated macrophages (TAMS) support the release of CSF-1 from tumors and Epidermal Growth Factor (EGF) from macrophages via paracrine signaling involving invading tumor cells.[14–16] The functions of macrophages are flexible, allowing them to transition from an M1 to an M2 polarization state to meet different physiological needs. M2 macrophages secrete type II cytokines, promoting the development of inflammation and tumorigenesis.[17,18] There is a need to enhance the indicators that facilitate identification of M2 macrophages phenotypes and to predict the prognosis in BC.

In this study, we used bioinformatics tools including a variety of databases to explore the prognostic significance of IFI44, to study the association of IFI44 with immune cells and to construct the significance of IMS. The ability of IFI44 to proliferate, migrate and invade was evaluated using cell viability, colony-formation assays and transwell tests in vitro, which provided evidence that IFI44 could enhance the expression of IL-10 and thereby enhance the infiltration of M2 macrophages. Survival curve, Receiver Operational Characteristic (ROC) and Pan Cancer Survival Curve were employed to verify the effectiveness of IMS in evaluating prognosis and achieving a good response in multiple validation datasets. Therefore, we demonstrated that IFI44 may be a potential immunotherapy target and that the IMS may help forecast chemotherapy response and outcomes in BC.

Materials and Methods

Acquisition and Processing of Data

Expression profiles containing 337 samples from GSE47994,100 samples from GSE36772 and 86 samples from GSE15852 were downloaded. Clinical profiling and corresponding characteristics for 2509 BC instances (METABRIC) were retrieved from cBioPortal. RNA expression profiling data for clinical and related genes for pan-cancer was obtained using the "Bioconductor" package in The Cancer Genome Atlas database (TCGA) biolinks (RNA SeqV2).[19] IFI44 expression in normal and breast cancer tissues was analyzed using immunohistochemistry data from the HPA database. The expression of IFI44 in multiple cell lines was obtained from the HPA database. Correlation between the IFI44 and IL-10 was explored by TIMER and GEPIA2.

Assessment of Immune Infiltration

Targeted therapy in cancer is closely related to the immune microenvironment.[20,21] The ESTIMATE algorithm (*estimation*) was employed to score the purity of the matrix, immunity, and tumor.[22] *CIBERSORT* was applied to estimate the relative fractions of immune cell types in GSE47994 and GSE36772.[23] The association between IFI44 levels and the infiltration of key immune cell types in GSE47994 and GSE36772 was evaluated using Spearman correlation.

Correlations Between IFI44 and M2 Marker Genes

Genes with connection to M2 macrophages infiltration were dug by the R packages "limma" and "tidyverse" with a significance level of $P < 0.01$ and an absolute $R > 0.2$ value above the defined threshold to look for marker genes.[24] The threshold of absolute $R > 0.2$ was chosen to include genes showing at least a weak-to-moderate association with M2 macrophage infiltration. The more stringent P-value threshold of <0.01 was applied to increase confidence in the selected markers. Then, Spearman's coefficient was employed to conduct expression correlation assays between IFI44 and M2 marker genes in the TCGA cohort.

Cell Culture and Transfections

To select appropriate cellular models for functional validation, we firstly examined the basal expression of IFI44 across breast cancer cell lines using the HPA database. This led us to choose HCC70 (high endogenous expression) and MDA-MB-231 (low endogenous expression) for subsequent loss- and gain-of-function studies, respectively. The HCC70 BC cells and MDA-MB-231, which obtained from Chinese Academy of Sciences, were cultured in the RPMI-1640 and DMEM medium, respectively. Short hairpin RNA (shRNA) of IFI44 and over-expression of IFI44 (OE) plasmids were obtained from GenePharma, and the plasmids were separately transfected into HCC70 cells and MDA-MB-231 cellls. The shRNA had the following sequences: shIFI44-1:5′-GCGAAGATTCACTGGATGAAA-3′, and shIFI44-2: 5′-CCCTGTAAAGGATGTTCTAAT-3′. Following the manufacturer's guidelines, shRNA transfection was carried out.[25] MDA-MB-231 was transfected with IFI44 plasmid that overexpresses genes.

Real-Time Quantitative

To verify the transfection efficiency of our constructed cell lines, RT-qPCR was used. Trizol (TaKaRa) was used to extract RNA from the MDA-MB-231 and HCC70 cells. The extracted RNA was transcribed into cDNA via the PrimeScript™ II Reverse Transcriptase (Servicebio). PCR amplification of the IFI44 strictly following the manufacturer's instructions (Servicebio). Primers were in the following manners: ACTIN, forward (F): 5′-CACCCAGCACAATGAAGATCAAGAT-3′, reverse (R): 5′-CCAGTTTTTAAATCCTGAGTCAAGC-3′; IFI44, forward (F): 5′-TCCAAGGGCATGTAACGCAT-3′, reverse (R): 5′-CCTCCCTTAGATTCCCTATTTGCT-3′. The levels of IFI44 mRNA were quantified relative to the ACTIN mRNA using the $2^{-\Delta\Delta Cq}$ method.

Cell Viability and Colony Formation Assays

To detect cell viability, the Cell Counting Kit-8 (CCK-8) from Beyotime (#C0037) was employed based on the instructions given by manufacturer. After 12 h transfection, HCC70 and MDA-MB-231cells were put into 96 well plates at 2000 cells density. A microplate reader was used to record absorption at 450 nm. Over a period of four days, each day's absorbance data is used to plot cell proliferation curves.[26] In the colony formation assay, 500 cells were seeded and cultured in 6-well plates until colonies became visible. 4% formalin fixation and 1% crystal violet were then used to stain and count the colonies.

Transwell Assays

Migration assays were performed with chamber (5-mm pore size, Corning) and invasion assays were supplemented with Matrigel (BD Biosciences). Twelve hours post-transfection, 50,000 cells were placed into the upper chambers using 200μL of medium without serum, and lower chamber only added 600μL of 10% FBS medium. The upper insert cells were transplanted to the lower surface, subsequently treated with 4% formalin and colored using 1% crystal violet, following a 24-hour culture period at 37 °C. The average number of tumor cells was counted in randomly selected microscope fields.

M2 Macrophage Infiltration Assay

The innate immune system plays a fundamental role in tumor immune surveillance and response to immunotherapy, with macrophage polarization directly influencing the immune balance within the tumor microenvironment.[27] THP-1, obtained from the Chinese Academy of Sciences, was seeded in 6-well plates using RPMI-1640 medium with 10% FBS. 100 ng/mL PMA was added for 12h to stimulate THP-1 differentiation to M0 macrophages when the density reached 5×10^5. M0 macrophages were polarized to M2 with 20ng/mL IL-4 (MedChemExpress) and 20ng/mL IL-13 (MedChemExpress) for 48h at 37°C.[28] 2.5×10^5 M2 macrophages that had been serum-free for a full 12 hours were seeded in chambers, and 2.5×10^5 MDA-MB-231 and HCC70 cells were planted in the lower chamber with 10% fetal bovine serum.[29] After incubation for totally 24 hours, 5% CO_2 concentration at 37°C, cells in the lower surface were fixed, stained and quantified.

Flow Cytometry

Cells collected from lower chamber of the Transwell assay are rinsed and incubated in the dark at 4°C for half an hour. The following anti-human antibodies were used: CD163-PE-Cy7(BD Biosciences); CD206-APC (BD Biosciences).[30] The results of positive CD163/CD206 were analyzed using the FlowJo 10.10 software program.

Elisa

IL-10 is a marker for M2 macrophages, and we wonder whether the expression of IFI44 would synchronously affect the expression of IL-10. In this study, IL-10 was quantitatively detected by double-antibody sandwich ELISA (Abcam, ab185986) based on the instructions given by manufacturer.

Patient Tissue Collection

Breast cancer tissues were obtained from 10 individuals, who suffered surgical treatment at the Department of Breast Disease Center, The First Affiliated Hospital of Nanchang. This study's clinical research protocol was supported from the Ethics Committee at Nanchang University, and the patients signed the informed consent. Tissues were swiftly frozen in liquid nitrogen and maintained at −80°C for later experiments.

Immunohistochemistry

IHC staining was used to assess the different levels of expression for IL-10 and IFI44 in clinical samples (n=10). Tissue sections were stained with 3, 3′-diaminobenzidine for signal detection. anti-IFI44 and anti-IL-10 antibodies were sourced from Proteintech.[31] Two seasoned pathologists conducted an independent examination and quantification of the image of sections.

Establishment and Confirming a Predictive Signature in BC

BC patients were split into training (TCGA) and testing (METABRIC) cohorts. The TCGA group was employed to identify IFI44-related M2 marker genes with prognostic significance by univariate and multivariate cox survival analysis. Using LASSO Cox regression by R package "*glmnet*", the final four genes were identified through multivariable cox analysis. The risk score=$\beta_1X_1 + \beta_2X_2 + \ldots + \beta_iX_i$. The formula employs X_i to denote the gene expression value from the predictive model, utilizing B_i as its respective coefficient.[32] Kaplan–Meier survival analysis categorized samples into different risk groups by median score. The prognostic model's predictive efficacy was confirmed via the ROC curve analysis, executed with the R "Time Roc" package. Moreover, for evaluation of the risk-model, the METABRIC cohort evaluated signature prognostic performance with this formula. Therefore, we used forest plots to comprehensively evaluate the risk model's precision by incorporating the nine clinical information: tumor size; lymph node states; age; menopausal state; ER; HER-2; Nottingham Prognostic Index (NPI); pathological grade and IMS score.

Susceptibility Analysis

Drug sensitivity testing utilized Cancer Drug Susceptibility Genomics 2 database (GDSC2)[33] and the relationship between IMS and drug susceptibility was explored using the "onco Predict" R software package.

Statistical Analysis

Data are presented as mean ± standard deviation (SD) from at least three independent experiments, each performed in triplicate (technical replicates). Student's t-tests were compared to groups with normal distribution, while the Wilcoxon rank-sum test assessed non-normal distributions, and visualize statistical results with GraphPad Prism Version 10. Via the application of cox regression, we meticulously examined the prognostic factors. Subsequently, leveraging the "survival" and "survminer" R packages, we crafted a robust prognostic model. The Kaplan-Meier curve was used for the analysis of survival data, and the association of clinical and pathological parameters with varying risk groups in BC patients was analyzed via the Chi-Square test. If the outcomes indicated that P was less than 0.05, it was considered statistically significant. *$p < 0.05$; **$p < 0.01$; ***$p < 0.001$ by Student's *t* test.

Results

IFI44 Demonstrated Increased Expression in BC and Related with Poor Prognosis

Evidence indicated elevated expression of IFI44 in HNSC tumors,[8] however, the expression of IFI44 in BC is unexploited. We examined the expression of IFI44 mRNA levels between tumor and normal samples in the TCGA and discovered that IFI44 was notably increased in several cancer types, including BRCA (Figure 1A). Then, our findings found that IFI44 demonstrated increased expression in paired BC tissues from TCGA and GSE15852 databases (Figure 1B and C). Immunohistochemistry from HPA showed that IFI44 was higher than that of normal tissues in BC tissues (Figure 1D). Thus, this study delved into the link between IFI44 expression and prognosis through the K-M plotter database, and we found that the prognosis of patients with increased expression of IFI44 was poor (Figure 1E).

IFI44 Promoted Proliferation, Migration, and Invasion of BC Cells

The role of IFI44 in breast cancer is unknown. In U87 and U251 cells, increased expression of IFI44 facilitated cell proliferation, movement, and invasiveness, whereas knockdown suppressed these phenotype.[34] We firstly assessed IFI44 mRNA levels by The Human Protein Atlas in multiple cell lines and found that IFI44 was highly expressed in HCC70 cell line, but low in MDA-MB-231 cell line (Figure 2A). By employing two specific shRNAs, we decreased IFI44 levels in HCC70 BC cells, transfected with IFI44 gene overexpression plasmid in MDA-MB-231 and validated by qRT-PCR (Figure 2B). Based on CCK-8 (Figure 2C), colony formation (Figure 2D) and transwell assays (Figure 2E), it had been presented to inhibit the proliferation and invasion of BC cells in HCC70 cells. However, overexpression of IFI44 in MDA-MB-231 promoted the ability of BC cells in proliferation, invasion, and metastasis (Figure 2F). Together, we have demonstrated that IFI44 facilitated BC cells to proliferate, migrate, and invade.

The Expression of IFI44 Was Strongly Associated with Immune Infiltrating Cells

Since IFI44 induces antiviral responses that is widely reported to be predominantly expressed in virus, there is clinical interest in investigating the function of IFI44 in immune microenvironment. We performed immune infiltration analysis

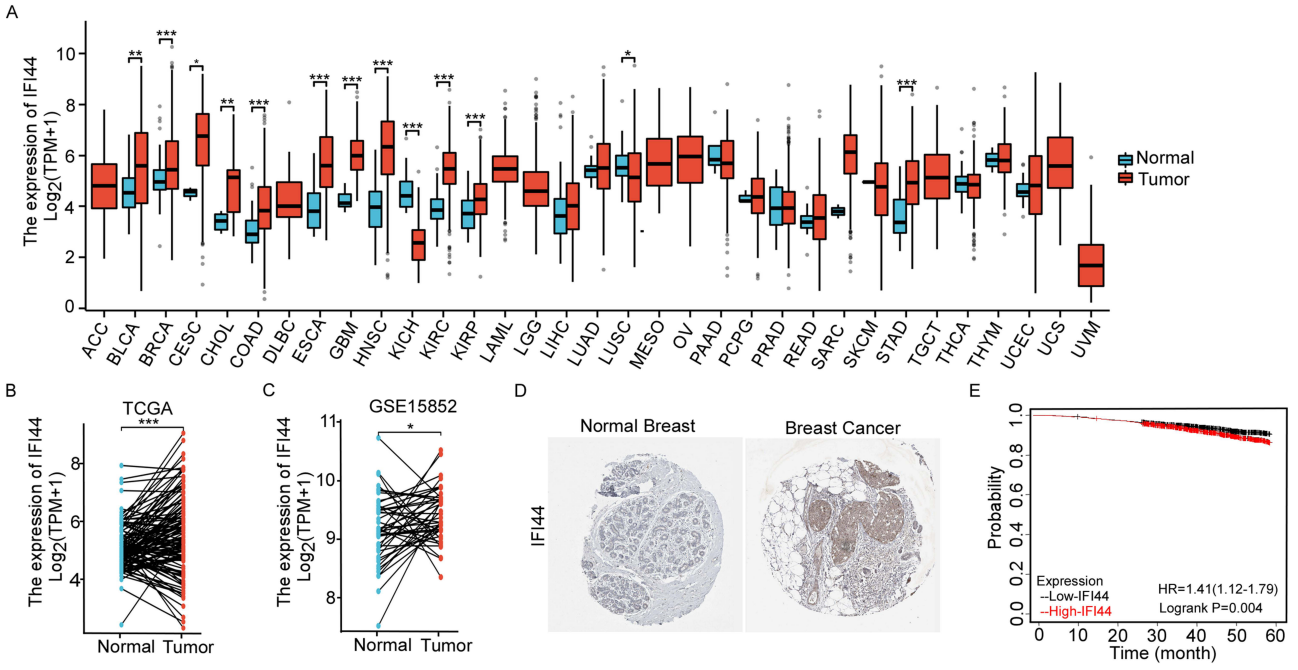

Figure 1 IFI44 was presented high expression in BC and linked to poor prognosis. (**A**) The expression of IFI44 between the normal and tumor tissues in various cancer types on the TCGA database. (**B** and **C**) The mRNA expression of IFI44 in the corresponding normal tissues from TCGA (n=4186) and GSE15852 (n=86) databases in BRCA. (**D**) The level of IFI44 protein expression in normal tissues and BC was identified from The Human Protein Atlas. (**E**) The Kaplan–Meier curves in patients. *p < 0.05; **p < 0.01; ***p<0.001.

https://doi.org/10.2147/BCTT.S579301

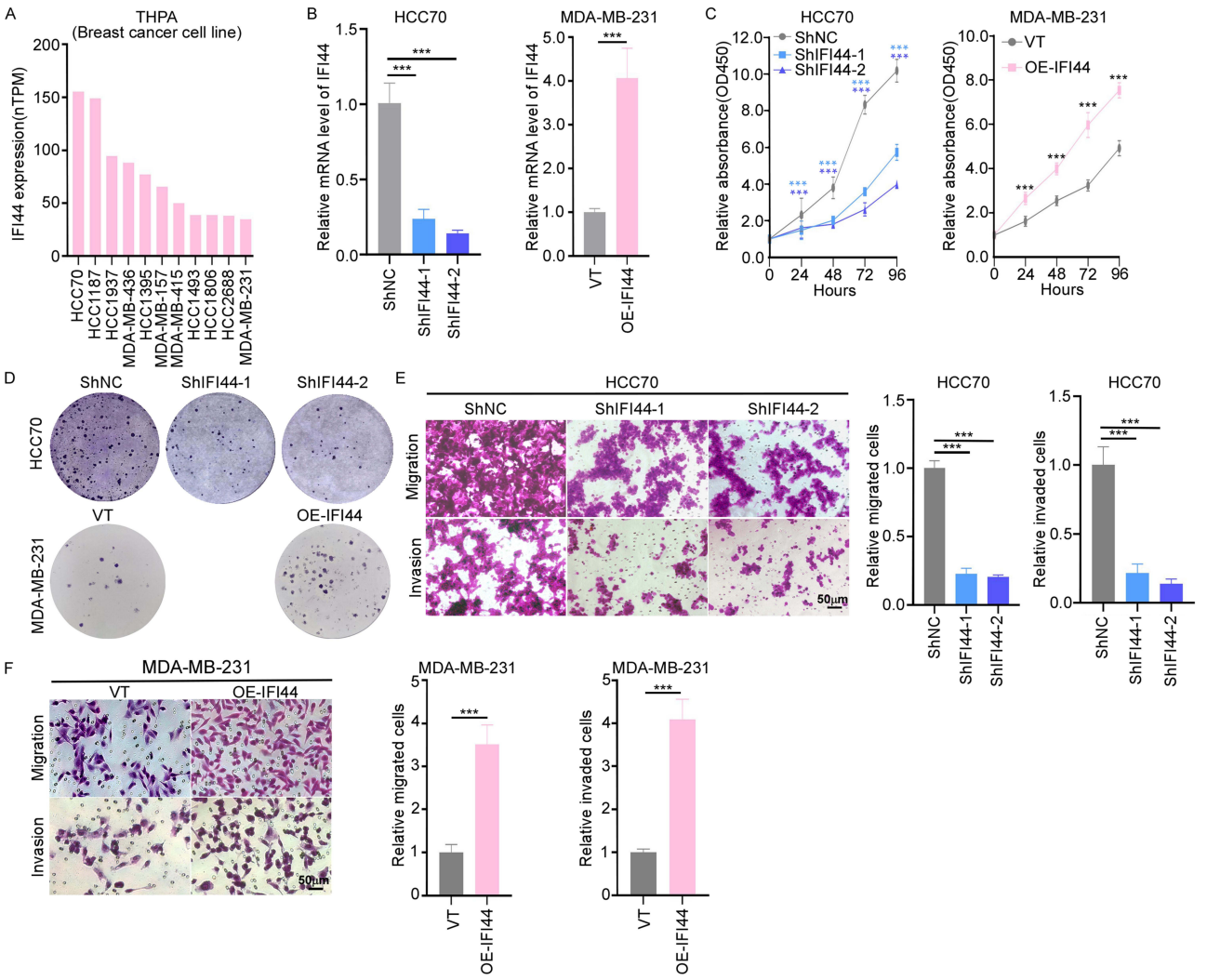

Figure 2 IFI44 promoted BC cell proliferation, migration, and invasion. (**A**) Difference in IFI44 mRNA expression between BC cell lines by The Human Protein Atlas. (**B**) The transfection efficiency of IFI44 shRNA and IFI44 overexpression in HCC70 and MDA-MB-231 by qRT-PCR. (**C** and **D**) The CCK8 and colony formation assays. (**E** and **F**) The transwell migration and invasion assays. ***p<0.001.

using *CIBERSORT* algorithm, thus exploring the potential association of IFI44 with immune cells in the GSE47994 and GSE36772 cohorts. In the GSE47994 cohort, we found that IFI44 was positively correlated with T cells CD8, Plasma cells, M2 Macrophage and M1 Macrophage, but negatively with T cells CD4 naive, NK cells activated, and monocytes (Figure 3A). The association between the IFI44 and immune cells was further evaluated in the GSE36772, and we found that the immune scores for M2 Macrophage and M1 Macrophage were increased in the group with elevated IFI44 than in the group with reduced IFI44 (Figure 3B). The trend of the results obtained by Spearman analysis is consistent (Supplementary Figure 1). Notably, M1 Macrophage and M2 Macrophage were discovered to be considerably more prevalent in the IFI44-high group in the GSE47994 and GSE36772 (Figure 3C). Thus, there may be interactions between the immune cell types and IFI44 that deserve future in-depth study.

High Expression of IFI44 in BC Promoted Infiltration of M2 Macrophages

Galectin-9 is highly expressed in the tumor microenvironment and binds to Tim-3 on the surface of macrophages, activating the PI3K/AKT signaling pathway, resulting in macrophage polarization to M2 type, which promotes tumor cell proliferation, movement, and invasiveness, thereby driving tumor development.[35] In order to explore whether IFI44 exerts pro-tumor function by regulating the tumor immune microenvironment, we first assessed the relationship between its expression and

https://doi.org/10.2147/BCTT.S579301

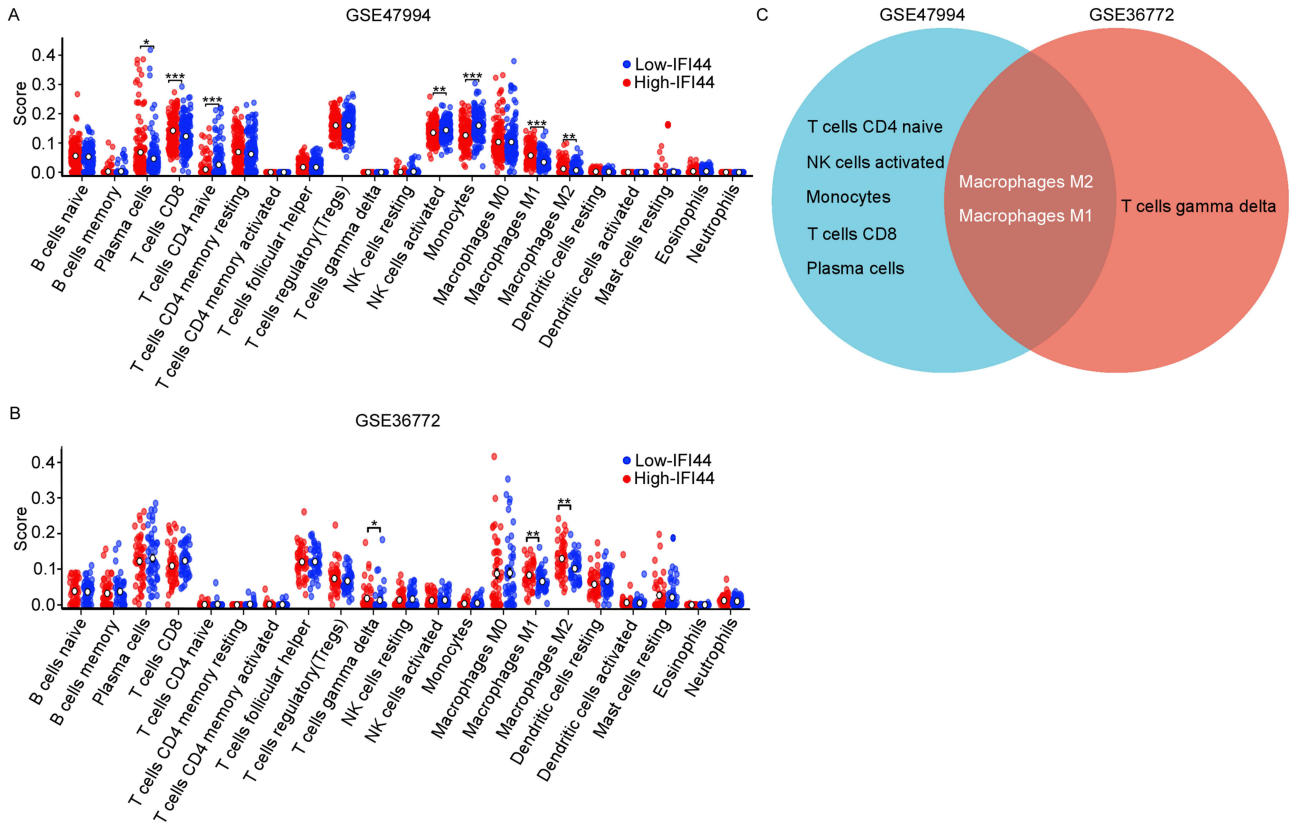

Figure 3 Characterization of IFI44 in BC microenvironment. (**A** and **B**) Immune infiltration cells in the GSE47994 (n=337) and GSE36772 groups (n=100). (**C**) Overlapping immune cell types showed a correlation with IFI44 expression across the two cohorts.*p < 0.05; **p < 0.01; ***p<0.001.

M2 infiltration. TIMER2 and GEPIA2 database correlation studies confirmed a sustained positive link between IFI44 and four M2 markers (IL10, CD163, TGFB1, and CSF1R), among which IL-10 was the most relevant (Figure 4A and B). Subsequently, IHC staining was used to evaluate the different levels of expression for IL-10 and IFI44 in clinical samples. Results indicated the expression trends of IFI44 and IL-10 were consistent with bio-information in BC (Figure 4C). To verify whether IFI44 can directly regulate M2 macrophage recruitment, we conducted in vitro co-culture experiments. Knocking down IFI44 in HCC70 cells resulted in less infiltration of M2 macrophages, but transwell experiments showed that the IFI44-OE group contained a significantly greater number of cells penetrating chambers in MDA-MB-231 and HCC70 cells (Figure 4D–F). Co-culture with IFI44-overexpressing tumor cells significantly increased the percentage of M2 macrophages ($CD206^+$, $CD163^+$). In addition, silencing IFI44 impaired the tumor cells' ability to promote M2 migration (Figure 4G). Elisa's results indicated that reduction of IFI44 expression in HCC70 cells attenuated the expression of IL-10. However, overexpression of IFI44 in 231 cells increased IL-10 expression (Figure 4H). Early studies had demonstrated that IL-10 signaling promotes the motility of M2 macrophages.[36] We speculated that IL-10 might contribute to the movement of M2 macrophages facilitated by IFI44. To verify the hypothesis, the number of M2 macrophages was examined in cells where IFI44 was silenced in HCC70 cell line and IFI44-OE in MDA-MB-231 cell line. As expected, low expression of IFI44 decreased the number the migration of M2 cells, but exogenous IL-10 application to the knockdown cells restored the diminished levels. Over-expression of IFI44 in MDA-MB-231 cells facilitated the movement of M2 macrophages; however, the addition of IL-10Ab inhibited the migration process (Figure 4I). Mechanistically, IFI44 orchestrates an IL-10–driven immunosuppressive microenvironment by enhancing M2 macrophage infiltration.

Construction of the IMS in the TCGA Set and Validation in the METABRIC Cohort

Considering the significant role of IFI44 and M2 macrophage in BC, it is important to formulate a model related to them to estimate the patients' prognosis with BC. Co-expression analysis identified 210 M2 marker genes, following filter

https://doi.org/10.2147/BCTT.S579301

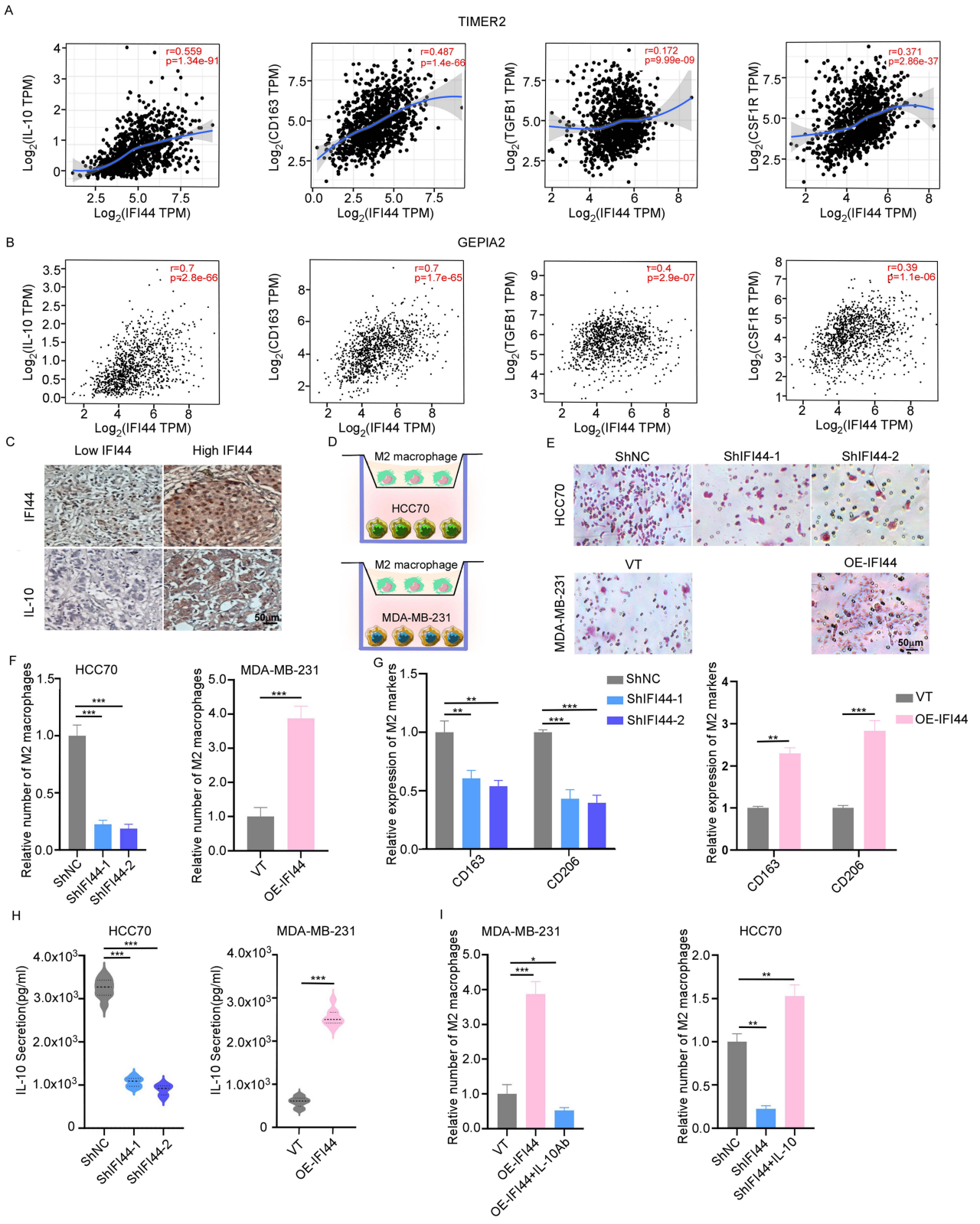

Figure 4 Impact of IFI44 on M2 Macrophage infiltration. (**A** and **B**) The association of IFI44 expression with M2 macrophage markers (IL-10, CD163, TGFB1, and CSF1R) based on TIMER2 and GEPIA2 database. (**C**) Immunohistochemical images of IFI44 and IL-10 high and low expression in BC tissues (n=10). (**D–F**) Infiltration of M2 macrophages in HCC70 cells and MDA-MB-231 cells. (**G**) Flow cytometric analysis for CD206 and CD163 expression in M2 macrophages after co-culture with HCC70 cells or MDA-MB-231 cells. (**H**) Assessment of IL-10 expression in HCC70 cells and MDA-MB-231 cells using Elisa. (**I**) Relative number of M2 macrophages in HCC70 cells and MDA-MB-231 cells with different treatment.* $p < 0.05$; ** $p < 0.01$; ***$p<0.001$.

https://doi.org/10.2147/BCTT.S579301

conditions with an absolute R above 0.2 and a p-value below 0.05 selected genes from the former 210 M2 marker genes, and identified the final 155 marker genes with a Pearson correlation coefficient's absolute value exceeds 0.2, with a p-value under 0.05. Then univariate cox regression analysis was used to identify 42 maker genes about OS, which were shown in the Heat Map (Figure 5A). Finally, the last 7 candidate genes were found using multivariate Cox regression model analysis, and subsequently applied to generate a forecast signature (Figure 5B). The LASSO regression analysis involved 7 genes to further suggest that 4 genes (GPR171, KIR2DS4, NPAS1 and CD79A) were identified when the cross-validation error reached its minimum (lambda. min=0.0079) (Figure 5C and D). The prognostic risk score based on IFI44 M2 signatures (IMS) was derived via the application of the given formula:

$$\text{IMS risk score} = (-0.0688)\times \text{GPR171} + (-0.2254)\times \text{KIR2DS4} + (-0.2209)\times \text{NPAS1} + (-0.0891)\times \text{CD79A}$$

This algorithm was used to calculate the risk in each BC patients and stratify the patients into various groups according to the median IMS risk score. This data demonstrated that there was a significantly higher mortality rate in high-risk patients compared to those at low risk (Figure 5E and F). The AUC of the ROC model for predicting the 1-year, 3-year, and 5-year survival of BC patients was 0.705, 0.698, and 0.614, respectively (Figure 5G). To test the validity of the model, we used a METEBIRC cohort to test its predictive performance, using a similar pattern to allocate patients to high- and low-risk cohorts. Consistent with the training cohort, patients in the high-risk group exhibited poorer OS than those in the low-risk group (Figure 5H). Thus, the outcomes of our research suggested that IMS risk score was highly specific and sensitive for predicting OS in BC patients.

The Clinical Value of IMS in BC

The IMS's status as a standalone predictive indicator was evaluated via a multivariate cox regression analysis, with covariates including tumor size, lymph node states, pausal state, ER-IHC, HER2-SNP6, NPI, tumor grade and IMS score. The analysis revealed that IMS had statistical significance in BC ($p \leq 0.001$) (Figure 6A), which further implied the IMS score model could act as an independent prognostic indicator for BC. Moreover, the value of IMS in the therapeutic effects of immunotherapy and chemotherapy in BC was explored. The ESTIMATE algorithm was utilized to derive the ESTIMATE score for every patient, indicating the comprehensive level of immune infiltration. In TCGA cohorts, low-IMS patients had elevated Stromal, Immune, and ESTIMATE scores relative to high-IMS patients ($P<0.001$, Figure 6B). Moreover, higher ESTIMATE scores might be associated with improved prognostic outcomes. We explored the association of IMS and the IC50 of certain anticancer drugs. As shown in Figure 6C, Cisplatin and Paclitaxel, which are frequently used anti-tumor drugs for TNBC in clinical settings, showed reduced effectiveness in high-IMS groups.

The Diagnostic Utility of This IMS with Pan-Cancer Analysis

To assess the value of IMS in Pan-cancer, we downed TCGA database's transcriptome expression profiles paired with clinical information for multiple cancer categories and calculated each sample's risk using a similar formula. To explore the prediction precision of the IMS in other cancers, a survival model was applied to investigate survival patterns across risk groups, with findings indicating notable differences among the stratifications illustrated by the IMS in four types (Bladder Urothelial Carcinoma (BLCA); HNSC; Skin Cutaneous Melanoma (SKCM); and Acute Myeloid Leukemia (LAML)) of cancer ($p\text{-value} \leq 0.05$) (Figure 7A and B). ESTIMATE's evaluation of immune infiltration showed a stark disparity can be observed between the high-IMS and low-IMS clusters across all four types of cancer, where the low-IMS clusters exhibit less immune system involvement (Figure 7C). The findings align with BRCA observations. Consequently, the results suggest that IMS could potentially be used for other cancers.

Discussion

IFI44 is activated, and linked to infections by various viruses,[6] including papillomavirus and influenza virus.[37] Nevertheless, there remains insufficient evidence regarding the role of IFI44 in BC. Here, we found that IFI44 overexpression was associated with unfavorable outcomes, presented potential for modulating the immune system, and the IFI44-based IMS independently predicted prognosis, highlighting its potential as a prognostic indicator. Cellular viability, clonogenic and transwell invasion studies were implemented in vitro to ascertain the function of IFI44,

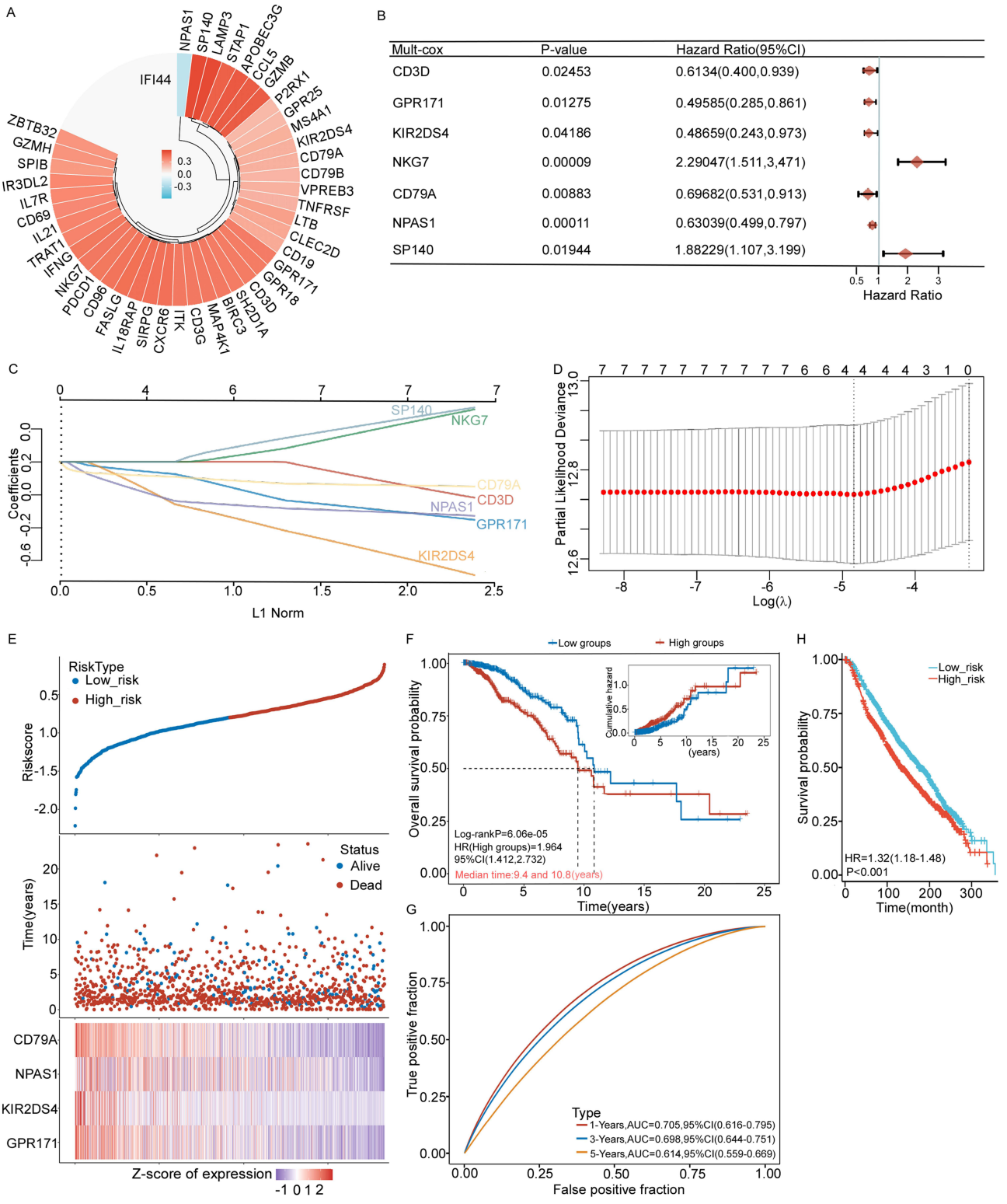

Figure 5 Construct and verify the accuracy of this IFI44-M2 signature in the TCGA and METABRIC cohorts. (**A**) Heat map showed the 42 M2 maker genes had a notable connection with IFI44. (**B**) Forest plots were created by analyzing candidate genes with multivariate methods, focusing on their association with BC patient survival rates in the TCGA cohorts (n=4186). (**C** and **D**) LASSO regression for the selection of characteristic parameters. (**E**–**G**) BC patient outcomes; distribution of risk scores and survival outcomes analysis for overall survival in the training cohorts. (**H**) BC patients' survival analysis in the validation cohorts.

https://doi.org/10.2147/BCTT.S579301

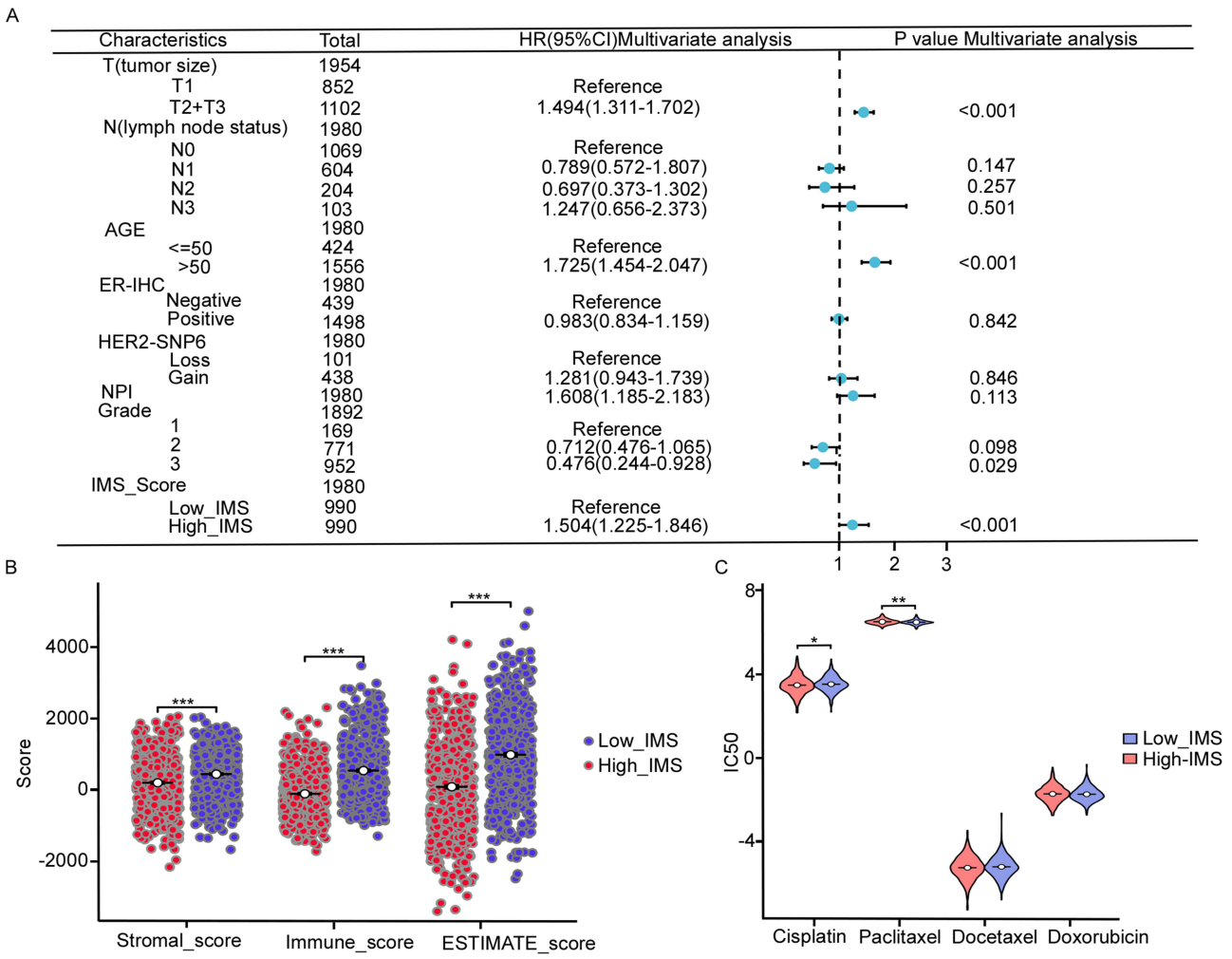

Figure 6 The clinical value of IMS in BC. (**A**) The IMS risk score was analyzed using multivariate cox regression in the METEBIRC cohorts (n=2509). (**B**) In the TCGA cohort, the scores were compared between high-risk and low-risk groups. (**C**) The IC50 measurements for five FDA-approved chemotherapeutic drugs in high-risk and low-risk categories of the TCGA cohort.*p < 0.05; **p < 0.01; ***p<0.001.

revealing its ability to enhance BC cell proliferation, movement, and invasion. Overall, IFI44 was found to be an elevated biomarker that was closely linked to unfavorable outcomes in BC.

Studies currently emphasize the influence of IFI44 on the INF-α/β mediated anti-viral process,[38] pathogenesis of SLE,[39] tumor radiation resistance[40] and neuroinflammation.[41] The possible roles of IFI44 in modulating the immune system during cancer development have been less explored. We investigated the potential association of IFI44 with immune cells by *CIBERSORT* algorithm, and IFI44 exhibited a positive association with M2 Macrophages in GSE47994 and GSE36772. The tumor microenvironment (TME) significantly influences cancer progression by utilizing tactics such as physical obstructions, cellular fatigue, a suppressed immune milieu and immune cells.[42,43] Macrophages fall into two primary types, M1 macrophages and M2 macrophages, playing distinct roles in immune response and monitoring. These cells are not set in stone but can switch between types depending on shifts in their surrounding conditions. M1 macrophages release proinflammatory cytokines that effectively combat pathogens, while M2 macrophages facilitate angiogenesis, tumor progression, and metastasis.[44] Correlation analyses revealed a positive connection between IFI44 and M2 macrophage abundance and markers a positive connection between IFI44 and M2 macrophage infiltration and markers, with IL-10 having the most significant positive relationship. Research indicated that IL-10, CD163, TGFB1, CSF1R, parasitic infections, and various stimulations promote macrophage polarization toward the M2 phenotype.[45,46] Via IL-10 signaling, IFI44 directed M2 macrophages to move towards BC cells. For instance, in pancreatic ductal

https://doi.org/10.2147/BCTT.S579301

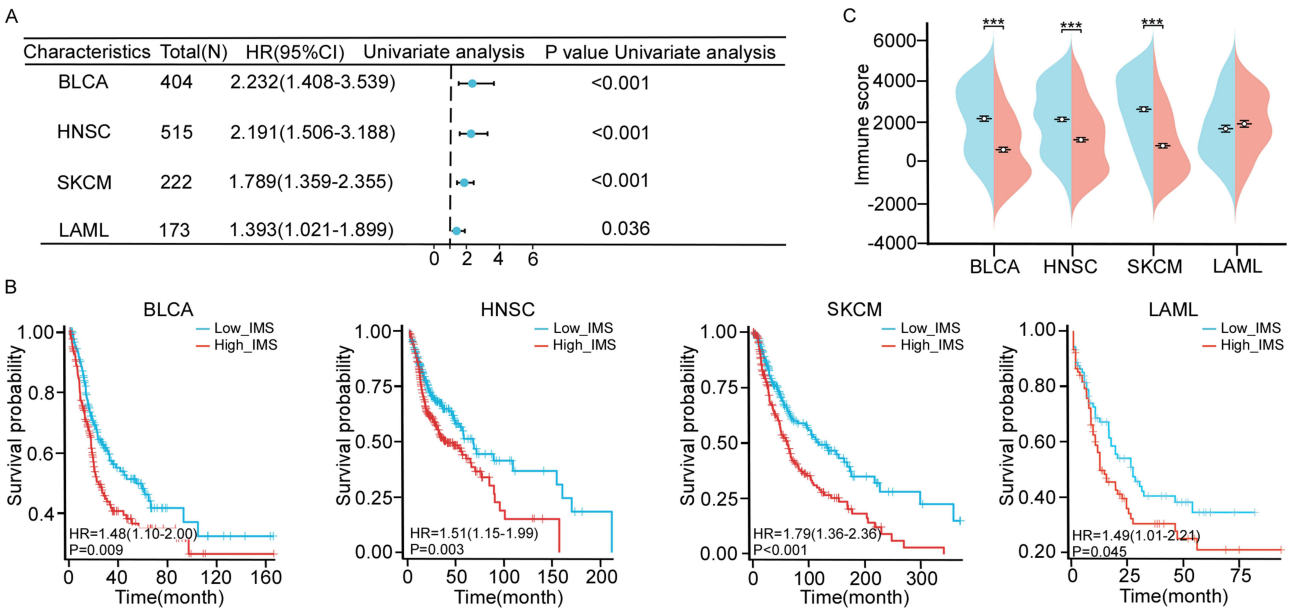

Figure 7 The clinical value of IMS in pan-cancer. (**A**) Validation of the IMS's effect on survival was conducted using TCGA pan-cancer datasets. (**B**) In five cancer types, KM-OS curves were analyzed between patients with elevated and reduced IMS scores. (**C**) Analyzing the relative distribution of ESTIMATE-derived immune scores in high- and low-risk groups for five types of cancer. ***p<0.001.

carcinoma, inhibiting the expression of key factors of M2 macrophages in the immune microenvironment, such as CD163, will significantly weaken the ability of tumors to invade and spread to distant sites.[47] However, increasing the M1/M2 macrophage ratio inhibits tumorigenicity.[48] These outcomes collectively demonstrated that IFI44 encouraged the trafficking of macrophages, their M2 polarization, and the motility of M2 macrophages towards BC cells, resulting in an immunosuppressive environment, which contributed significantly to the resistance against immunotherapy in BC.

Furthermore, we established a nomogram incorporating risk scores and clinical variables to predict survival probabilities, which confirmed the risk score as an independent prognostic indicator. To further certify the dependability of the IMS in pan-cancer, we acquired transcriptome expression datasets for various cancer types from the TCGA database and applied our formula to every patient. Several cancers, including BLCA, HNSC, SKCM and LAML, low-risk group members exhibited improved survival rates and greater immune score than those in the high-risk group. M2 macrophage-mediated immunosuppression represents a hallmark of the tumor microenvironment across multiple cancer types.[49–52] IFI44, as an interferon-stimulating gene, may be involved in shaping an immunosuppressive environment conducive to M2 polarization in these cancers. IL-10–Driven M2 Macrophage may participate in the immune regulation of these cancers, thus enabling IMS based on this axis to have cross-cancer prediction capabilities.

Current breast cancer immunotherapy faces the challenge of limited response rates and lack of precise biomarkers. The IFI44-IL-10-M2 axis identified in this study reveals a non-classical, intrinsically driven immunosuppressive mechanism by tumor cells, which may partly explain why some tumors are insensitive to existing immune checkpoint inhibitors. Therefore, targeting this axis is expected to provide new combination therapy ideas for overcoming drug resistance.

However, there are additional ideas that could be explored to enhance our research. Initially, mechanism exploration mainly relies on cell line models, which provide strong evidence for causality but may not fully simulate tumor heterogeneity and complex tumor-matrix-immune interaction networks in vivo. Secondly, our constructed IMS signatures and their associations with the immune microenvironment still need to be validated in more prospective clinical cohorts and multi-omics data containing fresh tissue samples. In addition, the limitation of this study is that IFI44 may affect the microenvironment through factors other than IL-10. In the future, through the cytokine profiling analysis of co-culture systems, its immunomodulatory network will be more comprehensively revealed. Overall, our findings not only provide

a new mechanistic viewpoint for understanding immune evasion in breast cancer, but also lays a theoretical foundation for the future development of combination immunotherapies based on IFI44 or tumor-associated macrophages.

Conclusion

In summary, our study demonstrates that IFI44 is an oncogenic driver in breast cancer that promotes proliferation, migration, and invasion of tumor cells. Mechanistically, IFI44 orchestrates an IL-10–driven immunosuppressive microenvironment by enhancing M2 macrophage infiltration. The IFI44-based M2 macrophage signature (IMS) we developed serves as a robust and independent prognostic indicator, capable of predicting patient survival and potential chemotherapy response. These findings not only elucidate a novel immune-regulatory role of IFI44 but also propose the IMS as a promising predictive tool for personalized therapy in breast cancer and potentially other malignancies.

Data Sharing Statement

Data is provided within the manuscript.

Ethics Approval and Consent to Participate

This study was performed in line with the principles of the Declaration of Helsinki. Approval was granted by the Ethics Committee of Nanchang University ((2024) CDYFYYLK (12-080)).

Acknowledgments

We thank all the members for participating in this study.

Author Contributions

All authors made a significant contribution to the work reported, whether that is in the conception, study design, execution, acquisition of data, analysis and interpretation, or in all these areas; took part in drafting, revising or critically reviewing the article; gave final approval of the version to be published; have agreed on the journal to which the article has been submitted; and agreed to be accountable for all aspects of the work.

Funding

This work was funded by the Science and Technology Plan Project of Jiangxi Provincial Administration of Traditional Chinese Medicine (2024A0196, 2024B1251).

Disclosure

The authors declare no competing interests.

References

1. Albuquerque C, Manguinhas R, Costa JG, et al. A narrative review of the migration and invasion features of non-small cell lung cancer cells upon xenobiotic exposure: insights from in vitro studies. *Transl Lung Cancer Res*. 2021;10(6):2698–2714. doi:10.21037/tlcr-21-121
2. Arnold M, Morgan E, Rumgay H, et al. Current and future burden of breast cancer: global statistics for 2020 and 2040. *Breast*. 2022;66:15–23. doi:10.1016/j.breast.2022.08.010
3. Waks AG, Winer EP. Breast cancer treatment: a review. *JAMA*. 2019;321(3):288. doi:10.1001/jama.2018.19323
4. Ge J, Zuo W, Chen Y, Shao Z, Yu K. The advance of adjuvant treatment for triple-negative breast cancer. *Cancer Biol Med*. 2021;18:1. doi:10.20892/j.issn.2095-3941.2020.0752
5. Narote S, Desai SA, Patel VP, Deshmukh R, Raut N, Dapse S. Identification of new immune target and signaling for cancer immunotherapy. *Cancer Genetics*. 2025;294–295:57–75. doi:10.1016/j.cancergen.2025.03.004
6. Kitamura A, Takahashi K, Okajima A, Kitamura N. Induction of the human gene for p44, a hepatitis-C-associated microtubular aggregate protein, by interferon-α/β. *Eur J Biochem*. 1994;224(3):877–883. doi:10.1111/j.1432-1033.1994.00877.x
7. Honda Y, Kondo J, Maeda T, et al. Isolation and purification of a non-a, non-B hepatitis-associated microtubular aggregates protein. *J Gen Virol*. 1990;71(9):1999–2004. doi:10.1099/0022-1317-71-9-1999
8. Pan H, Wang X, Huang W, et al. Interferon-induced protein 44 correlated with immune infiltration serves as a potential prognostic indicator in head and neck squamous cell carcinoma. *Front Oncol*. 2020;10:557157. doi:10.3389/fonc.2020.557157
9. Shimizu YK, Oomura M, Abe K, et al. Production of antibody associated with non-a, non-B hepatitis in a chimpanzee lymphoblastoid cell line established by in vitro transformation with epstein-barr virus. *Proc Natl Acad Sci U S A*. 1985;82(7):2138–2142. doi:10.1073/pnas.82.7.2138

10. DeDiego ML, Nogales A, Martinez-Sobrido L, Topham DJ, Moscona A. Interferon-induced protein 44 interacts with cellular FK506-binding protein 5, negatively regulates host antiviral responses, and supports virus replication. *mBio*. 2019;10(4):e01839–19. doi:10.1128/mBio.01839-19
11. Walters K-A, Smith MW, Pal S, et al. Identification of a specific gene expression pattern associated with HCV-induced pathogenesis in HCV- and HCV/HIV-infected individuals. *Virology*. 2006;350(2):453–464. doi:10.1016/j.virol.2006.02.030
12. Yq C, Sb W, Jh L, et al. Modifying the tumour microenvironment and reverting tumour cells: new strategies for treating malignant tumours. *Cell Proliferation*. 2020;53(8):12865 doi:10.1111/cpr.12865
13. Chen M, Lai R, Lin X, Chen W, Wu H, Zheng Q. Downregulation of triggering receptor expressed on myeloid cells 1 inhibits invasion and migration of liver cancer cells by mediating macrophage polarization. *Oncol Rep*. 2021;45(4):37. doi:10.3892/or.2021.7988
14. Liang Z-W, Ge -X-X, Xu M-D, et al. Tumor-associated macrophages promote the metastasis and growth of non-small-cell lung cancer cells through NF-κB/PP2Ac-positive feedback loop. *Cancer Sci*. 2021;112(6):2140–2157. doi:10.1111/cas.14863
15. Pyonteck SM, Akkari L, Schuhmacher AJ, et al. CSF-1R inhibition alters macrophage polarization and blocks glioma progression. *Nat Med*. 2013;19(10):1264–1272. doi:10.1038/nm.3337
16. Wolfsberger J, Sakil HAM, Zhou L, et al. TAp73 represses NF-κB-mediated recruitment of tumor-associated macrophages in breast cancer. *Proc Natl Acad Sci U S A*. 2021;118(10):e2017089118. doi:10.1073/pnas.2017089118
17. Weiskopf K, Weissman IL. Macrophages are critical effectors of antibody therapies for cancer. *MAbs*. 2015;7(2):303–310. doi:10.1080/19420862.2015.1011450
18. Zhou J, Tang Z, Gao S, Li C, Feng Y, Zhou X. Tumor-associated macrophages: recent insights and therapies. *Front Oncol*. 2020;10:188. doi:10.3389/fonc.2020.00188
19. Chong W, Shang L, Liu J, et al. m6A regulator-based methylation modification patterns characterized by distinct tumor microenvironment immune profiles in colon cancer. *Theranostics*. 2021;11(5):2201–2217. doi:10.7150/thno.52717
20. Zheng D, Yan J, Liu X, et al. Artesunate nanoplatform targets the serine-MAPK axis in cancer-associated fibroblasts to reverse photothermal resistance in triple-negative breast cancer. *Adv Mater*. 2025;37(35):e2502617. doi:10.1002/adma.202502617
21. Xiao Y, Xu Y, Wang H, et al. HEBP2-governed glutamine competition between tumor and macrophages dictates immunotherapy efficacy in triple-negative breast cancer. *Cell Metab*. 2025;37(10):2030–2047.e7. doi:10.1016/j.cmet.2025.08.009
22. Vincent KM, Findlay SD, Postovit LM. Assessing breast cancer cell lines as tumour models by comparison of mRNA expression profiles. *Breast Cancer Res*. 2015;17(1):114. doi:10.1186/s13058-015-0613-0
23. Zhou R, Zhang J, Zeng D, et al. Immune cell infiltration as a biomarker for the diagnosis and prognosis of stage I-III colon cancer. *Cancer Immunol Immunother*. 2019;68(3):433–442. doi:10.1007/s00262-018-2289-7
24. Kim Y, Kang JW, Kang J, et al. Novel deep learning-based survival prediction for oral cancer by analyzing tumor-infiltrating lymphocyte profiles through CIBERSORT. *Oncoimmunology*. 2021;10(1):1904573. doi:10.1080/2162402X.2021.1904573
25. Andersen ND, Monahan TS, Malek JY, et al. Comparison of gene silencing in human vascular cells using small interfering RNAs. *J Am Coll Surg*. 2007;204(3):399–408. doi:10.1016/j.jamcollsurg.2006.12.029
26. Wang R, Gao X, Xie L, Lin J, Ren Y. METTL16 regulates the mRNA stability of FBXO5 via m6A modification to facilitate the malignant behavior of breast cancer. *Cancer Metab*. 2024;12(1):22. doi:10.1186/s40170-024-00351-5
27. Peng C, Feng Z, Ou L, et al. Syzygium aromaticum enhances innate immunity by triggering macrophage M1 polarization and alleviates helicobacter pylori-induced inflammation. *Journal of Functional Foods*. 2023;107:105626. doi:10.1016/j.jff.2023.105626
28. Phi LTH, Cheng Y, Funakoshi Y, et al. AXL promotes inflammatory breast cancer progression by regulating immunosuppressive macrophage polarization. *Breast Cancer Res*. 2025;27(1):70. doi:10.1186/s13058-025-02015-8
29. Xu Z, Chen X, Song L, Yuan F, Yan Y. Matrix remodeling-associated protein 8 as a novel indicator contributing to glioma immune response by regulating ferroptosis. *Front Immunol*. 2022;13:834595. doi:10.3389/fimmu.2022.834595
30. Wang Y, Lyu Z, Qin Y, et al. FOXO1 promotes tumor progression by increased M2 macrophage infiltration in esophageal squamous cell carcinoma. *Theranostics*. 2020;10(25):11535–11548. doi:10.7150/thno.45261
31. Yan Y, Xu Z, Qian L, et al. Identification of CAV1 and DCN as potential predictive biomarkers for lung adenocarcinoma. *Am J Physiol Lung Cell Mol Physiol*. 2019;316(4):L630–L643. doi:10.1152/ajplung.00364.2018
32. Shi Y, Xu Y, Xu Z, et al. TKI resistant-based prognostic immune related gene signature in LUAD, in which FSCN1 contributes to tumor progression. *Cancer Lett*. 2022;532:215583. doi:10.1016/j.canlet.2022.215583
33. Geeleher P, Cox N, Huang RS. pRRophetic: an R package for prediction of clinical chemotherapeutic response from tumor gene expression levels. *PLoS One*. 2014;9(9):e107468. doi:10.1371/journal.pone.0107468
34. Jin D, Mao L, Wu Y, Tang T, Yan E, Song Z. Unveiling the prognostic and immunological role of IFI44 in glioma. *Ann Med*. 2025;57(1):2593209. doi:10.1080/07853890.2025.2593209
35. Zhang J, Xu Y, Han X, Gao Y, Wei Z, Sun X. Galectin-9 promotes colon cancer development by polarizing macrophages toward the M2 phenotype. *Cancer Genet*. 2025;298–299:141–150. doi:10.1016/j.cancergen.2025.09.006
36. Li J, Liu Z, Wu X, et al. Anti-metastatic effects of AGS-30 on breast cancer through the inhibition of M2-like macrophage polarization. *Biomed Pharmacother*. 2024;172:116269. doi:10.1016/j.biopha.2024.116269
37. Kaczkowski B, Rossing M, Andersen DK, et al. Integrative analyses reveal novel strategies in HPV11,-16 and −45 early infection. *Sci Rep*. 2012;2:515. doi:10.1038/srep00515
38. Pasieka TJ, Baas T, Carter VS, Proll SC, Katze MG, Leib DA. Functional genomic analysis of herpes simplex virus type 1 counteraction of the host innate response. *J Virol*. 2006;80(15):7600–7612. doi:10.1128/JVI.00333-06
39. Nzeusseu Toukap A, Galant C, Theate I, et al. Identification of distinct gene expression profiles in the synovium of patients with systemic lupus erythematosus. *Arthritis Rheum*. 2007;56(5):1579–1588. doi:10.1002/art.22578
40. Khodarev NN, Beckett M, Labay E, Darga T, Roizman B, Weichselbaum RR. STAT1 is overexpressed in tumors selected for radioresistance and confers protection from radiation in transduced sensitive cells. *Proc Natl Acad Sci U S A*. 2004;101(6):1714–1719. doi:10.1073/pnas.0308102100
41. Brem R, Oraszlan-Szovik K, Foser S, Bohrmann B, Certa U. Inhibition of proliferation by 1-8U in interferon-alpha-responsive and non-responsive cell lines. *Cell Mol Life Sci*. 2003;60(6):1235–1248. doi:10.1007/s00018-003-3016-9
42. Kankeu Fonkoua LA, Sirpilla O, Sakemura R, Siegler EL, Kenderian SS. CAR T cell therapy and the tumor microenvironment: current challenges and opportunities. *Mol Ther Oncolytics*. 2022;25:69–77. doi:10.1016/j.omto.2022.03.009

43. Togashi Y, Shitara K, Nishikawa H. Regulatory T cells in cancer immunosuppression - implications for anticancer therapy. *Nat Rev Clin Oncol*. 2019;16(6):356–371. doi:10.1038/s41571-019-0175-7
44. Arnold CE, Whyte CS, Gordon P, Barker RN, Rees AJ, Wilson HM. A critical role for suppressor of cytokine signalling 3 in promoting M1 macrophage activation and function in vitro and in vivo. *Immunology*. 2014;141(1):96–110. doi:10.1111/imm.12173
45. Sica A, Larghi P, Mancino A, et al. Macrophage polarization in tumour progression. *Semin Cancer Biol*. 2008;18(5):349–355. doi:10.1016/j.semcancer.2008.03.004
46. Jenkins SJ, Ruckerl D, Thomas GD, et al. IL-4 directly signals tissue-resident macrophages to proliferate beyond homeostatic levels controlled by CSF-1. *J Exp Med*. 2013;210(11):2477–2491. doi:10.1084/jem.20121999
47. Liu Y, Wang X, Zhu Y, et al. The CTCF/LncRNA-PACERR complex recruits E1A binding protein p300 to induce pro-tumour macrophages in pancreatic ductal adenocarcinoma via directly regulating PTGS2 expression. *Clin Transl Med*. 2022;12(2):e654. doi:10.1002/ctm2.654
48. Silva KMR, França DCH, de Queiroz AA, et al. Polarization of melatonin-modulated colostrum macrophages in the presence of breast tumor cell lines. *Int J Mol Sci*. 2023;24(15):12400. doi:10.3390/ijms241512400
49. Jiang H, Liang L, Liu T, et al. A novel prognostic signature integrating disulfidptosis- and ferroptosis-related genes in acute myeloid leukemia. *Clin Exp Med*. 2025;25(1):303. doi:10.1007/s10238-025-01670-7
50. Suman S, Nevala WK, Leontovich AA, et al. Melanoma-derived extracellular vesicles induce CD36-mediated pre-metastatic niche. *Biomolecules*. 2024;14(7):837. doi:10.3390/biom14070837
51. Wu S, Lv X, Wei H, et al. Integrated analysis of single-cell RNA-seq and bulk RNA-seq unravels the molecular feature of M2 macrophages of head and neck squamous cell carcinoma. *J Cell Mol Med*. 2024;28(5):e18083. doi:10.1111/jcmm.18083
52. Xu Y, Chen D, Shen L, Huang X, Chen Y, Su H. Identification and mechanism of the PD-1/PD-L1 genomic signature SORL1 as protective factor in bladder cancer. *Front Genet*. 2021;12:736158. doi:10.3389/fgene.2021.736158